Defense Technical Information Center Compilation Part Notice

ADP012365

TITLE: CFD Simulation of Liquid Rocket Engine Injectors. Part 2. Simulations of the RCM-2 Experiment

DISTRIBUTION: Approved for public release, distribution unlimited

This paper is part of the following report:

TITLE: 2nd International Workshop on Rocket Combustion Modeling: Atomization, Combustion and Heat Transfer held in Lampoldshausen, Germany on 25-27 Mar 2001

To order the complete compilation report, use: ADA402618

The following component part numbers comprise the compilation report:
ADP012355 thru ADP012373

CFD SIMULATION OF LIQUID ROCKET ENGINE INJECTORS
Part 2. SIMULATIONS OF THE RCM-2 EXPERIMENT

Richard Farmer & Gary Cheng
SECA, Inc.

Yen-Sen Chen
ESI, Inc.

The sub-critical combustion case, RCM-2, was simulated with both heterogeneous and homogeneous spray combustion models. The MASCOTTE test data should be better than any which have been previously used to tune the several parameters in these models. It is unreasonable to expect that spray flames, even of hydrogen and oxygen, can be accurately predicted without extensive model validation with test data representative of the conditions which exists in rocket engine combustion chambers. Even global data such as chamber pressure and thrust have not been obtained for single coaxial element combustor flows. The IWRCM data provide a good starting point, but no CFD model tuning has yet been attempted for such experiments. Direct comparisons of predictions to test data at this point will not establish which of several modeling techniques is best.

Heterogeneous Spray Combustion Model

Simulations of shear coaxial injector combustion may include models that characterize the breakup or atomization of the round liquid jet, subsequent droplet secondary breakup, turbulence dispersion, droplet evaporation and gas-phase mixing and combustion. The primary atomization rate of the liquid jet is modeled following the work of Reitz and Diwakar[1]. Applications of this model to shear coaxial injector test cases, with a volume-of-fluid equation to model the liquid fuel/oxidizer jets, were presented by Chen, et al.[2]. For the present application, since the liquid core length and the initial droplet size are specified, the primary atomization model is therefore ignored.

Particulate Two-Phase Flow Model

The two-phase interactions are important throughout the life history of the droplets. In the initial phase of injection, momentum and energy exchanges through the drag forces and heat transfer are dominating. These inter-phase transfer terms appear in the Navier-Stokes equations that are solved using the present CFD flow solver. Mass transfer occurs as the particles are heated through the surrounding hot gas. Mean gas-phase properties and turbulence eddy properties are used for the statistical droplet tracking calculations.

Droplet Secondary Breakup Model

The TAB (Taylor Analogy Breakup) model of O'Rouke and Amsden[3] is based on an analogy between an oscillating and distorting droplet and a spring-mass system. The restoring force of the spring is analogous to the surface tension forces on the droplet surface. The external force on the mass is analogous to the gas aerodynamic force. The damping forces due to liquid viscosity are introduced also based on this model.

Droplet-Turbulence Interaction

A two-equation turbulence model is used to characterize the flowfield turbulence quantities, such as turbulence fluctuations, eddy life time and length scale. Turbulent effects on particles are modeled by assuming the influence of velocity fluctuations on the particles creates statistical dispersion of the particles. The velocity fluctuations, which are calculated from the solutions of the turbulence kinetic energy, are assumed to follow a Gaussian distribution with standard deviation proportional to the square root of turbulence kinetic energy. This magnitude of this statistical particle dispersion is then transported following the trajectory of the particles with their radii of influence within which coupling effects (also follow the Gaussian distribution) between two phases occur. This method is classified as the parcel PDF (cloud) model, by Shang[4], for turbulent particle dispersion. As oppose to the stochastic separated flow (SSF) model, the number of computational particles required is drastically reduced for the same statistical representation of the spray. This provides great savings in computational effort in performing the spray combustion computations.

Droplet Evaporation Model

The droplet evaporation rates and the droplet heat-up rates are determined using the general evaporation model of Schuman[5], which is continuously valid from subcritical to supercritical conditions. This vaporization model was extended from the classical approach[6], by neglecting the effects of solubility of the surrounding gas into the droplet. However, this approach satisfies the global transient film continuity equation for the drop vapor and the ambient gas to obtain the expressions consistent for the molar flow rates.

Chemical Reaction Model

A finite-rate chemistry model with point-implicit integration method is employed in the present study. A 9-reaction kinetics model of Anon[7] is used for modeling the H_2-O_2 combustion. The initiation reaction used produced OH. This chemistry model is listed in Table 1 of Part 3 of this paper.

Results

The MASCOTTE single injector test chamber was used in a series of experimental programs for subcritical and/or supercritical H_2-O_2 combustion. In the subcritical spray combustion test case (RCM-2), the designed chamber pressure is 10 bar (or 9.87 atm). The injector orifice diameter for the liquid oxygen (LOX) injection is 5 mm surrounded by an annular gaseous hydrogen jet with channel width of 6.4 mm. The overall O/F ratio for this case is 2.11 (see the test conditions given in Table 1).

Table 1. RCM-2 Test Case Operating Conditions

Conditions	H_2	O_2
Pressure	1 MPa	1 MPa
Mass flow rate	23.7 g/s	50 g/s
Temperature	287 K	85 K
Density	0.84 kg/m3	1170 kg/m^3
Cp	14300 J/kg/K	1690 J/kg/K
Velocity	319 m/s	2.18 m/s
Viscosity	8.6E-6 kg/m/s	1.94E-4 kg/m/s
Surface Tension	-	1.44E-2 N/m

The computational model includes the injector geometry, the combustion chamber and the nozzle section. A 10-block structured mesh is generated (the total number of grid points equals 14,444) for the two-phase flow computation. Relative high grid density (about 10 micron spacing)is packed in the injector lip region for the purpose of better flow resolution and flame holding in the expected area. The LOX core length of 7.8 mm is assumed, which serves as the particle injection boundary with the fixed particle size (82 microns), velocity (10 m/s) and angle distributions given in the problem specification. Fixed mass-flow boundary conditions are used at the inlet while all flow properties are extrapolated at the nozzle exit. Supersonic exit flow develops as part of the solution.

The computation starts with a cold flow with inlet and chamber pressure specified. The two-phase flow particle breakup and evaporation model models are activated from the beginning. The time step size of the time-marching solution method is 1 μsec. After 1000 time steps of cold flow run, a heat source is introduced in the lip region between and oxygen and hydrogen streams where a recirculation zone is established. At the same time, the finite-rate chemistry model is turned on to start the flame spreading throughout the chamber. The chamber pressure drops at the beginning until the flame fills up the entire chamber. Then, the pressure started to build up to the expected level when the inlet and exit flows show satisfactory mass conservation condition. The calculated averaged chamber pressure is around 9.96 atm. The majority of the LOX particles do not survive very far downstream of the injector exit. Some particles along the chamber axis do survive up to 70 mm downstream of the injector.

The time-averaged temperature, temperature standard deviation, species mass-fraction contours and temperature profiles at specified locations are plotted in the following figures. These data are prepared as requested for data comparison purpose.

Figure 1 shows the mean temperature and standard deviation through the entire length of the combustion chamber. A close up view of the nozzle tip region is also shown in this figure. Figure 2 shows the OH and O_2 and Figure 3 the H_2 and H_2O concentration profiles, respectively, in this same region. Figure 4 shows the predicted radial temperature profiles at various axial locations. Figure 5 shows the predicted axial temperature profiles at various radial locations. The flame predicted using this model does not expand as indicated in the experiment. The recirculation zone is relatively long.

Homogeneous Spray Combustion Model

The RCM-2 experiment was also simulated with the homogeneous spray combustion model. Details of this model are presented in Part 3 of this paper. The volume upstream of the injector element tip was neglected for this simulation. The grid use for the internal element flow was 61x43; for the chamber it was 301x101. The nozzle was not simulated. This grid system had a minimum grid spacing of 60 microns in the wake behind the lip separating the LOX and hydrogen streams. The boundary conditions used are shown in Figure 6. An equilibrium and several finite rate solutions were obtained for this configuration. An initial finite-rate simulation was run by setting the rate of the global initiation reaction fast enough to stabilize the flame near the start of the shear layer. This rate also essentially eliminated the waviness in the shear layer separating the LOX and hydrogen streams, without averaging the solution. The stoichiometric coefficients in the global rate expression were determined by an equilibrium calculation for a stoichiometric flame at the expected chamber pressure.

Such a practice produces temperatures with one rate expression, which are very close to those resulting from using a more detailed reaction mechanism. However, predicted OH concentrations are apparently too high. The procedure used in the case 3 simulation is believed to be much better. This modified procedure uses nine elementary rate equations and switches to an equilibrium solution when the local temperature exceeds a specified value. Temperatures and OH concentrations are believed to be accurately simulated by this method.

The equilibrium solution at the interface between the internal element flow and the flow at the nozzle tip are shown in Figure 7. The temperature profiles in the radial and axial directions are shown in Figures 8 and 9, respectively. The temperature and oxygen and OH concentration profiles are shown in Figure 10. The wall temperature profile is shown in Figure 11. All of these figures are for the equilibrium solution. The modified finite rate solution for the equilibrium/finite-rate combustion model yielded solutions very similar to the equilibrium only model. This modified finite-rate model is believed to be the most accurate and useful model tested.

Comparing the heterogeneous and homogeneous solutions, the former produced a longer, thinner flame than the latter. Parameters in the spray combustion model could have been set such that the solutions matched very closely, or so that both could match test data. Such a step cannot be made until the RCM test data are made available and the CFD models tuned. An optimum rocket engine spray combustion model cannot be determined until this next validation step is undertaken.

REFERENCES

1. Reitz, R. D., and Diwakar, R., "Structure of High-Pressure Fuel Sprays," SAE Paper 860469, 1986.
2. Chen, Y. S., Shang, H. M., and Liaw, P., "A Fast Algorithm for Transient All-Speed Flows and Finite-Rate Chemistry," AIAA Paper 96-4445, 1996 AIAA Space Programs and Technologies Conference, September 24-26, 1996, Huntsville, AL.
3. O'Rourke, P. J., and Amsden, A. A., "The TAB Method for Numerical Calculation of Spray Droplet Breakup," SAE Paper 872089, 1987.
4. Shang, H. M., "Numerical Studies of Spray Combustion in Liquid-Fueled Engines," Ph.D. Thesis, University of Alabama in Huntsville, 1992.
5. Schuman, M. D., "General Evaporation Model," CDR-88-054, Rockwell International Corp., Feb. 1988.
6. Abramzon, B., and Sirignano, W. A., "Droplet Vaporization Model for Spray Combustion Calculations," AIAA Paper 88-0636, 1988.
7. Anon, "Spray Combustion of Synthetic Fuels, Phase II – Spray Combustion Phenomena," DOE/PC40276-5, SAI, Inc., Chatsworth, CA, May 1983.

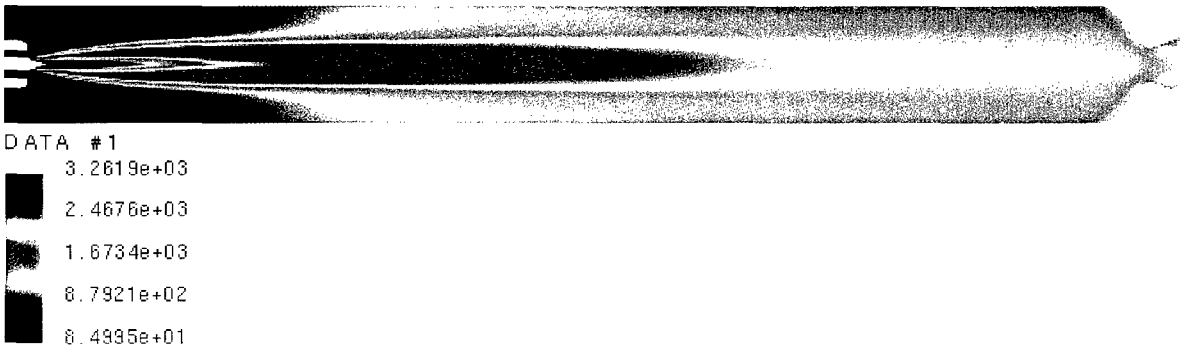

(a) Time-Averaged Temperature (K)

(b) Temperature Standard Deviation (K)

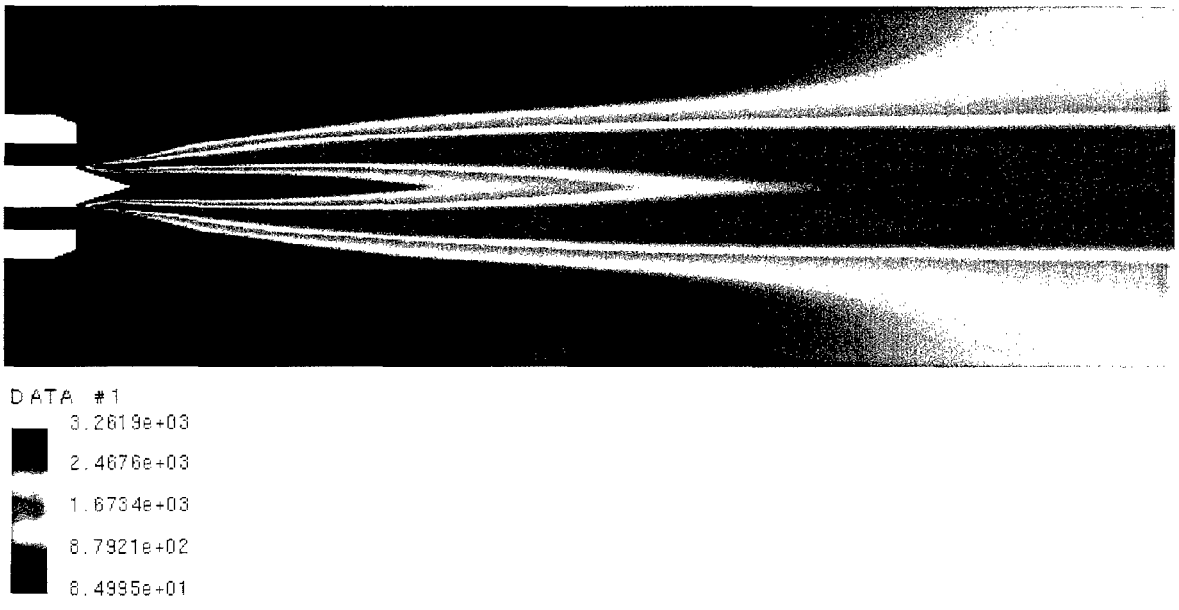

(c) Time-Averaged Temperature (K) for X up to 150 mm

Figure 1. Time-Averaged Temperature and Temperature Standard Deviation of RCM-2.

(a) Time-Averaged OH Mass-Fraction Contours for X up to 150 mm

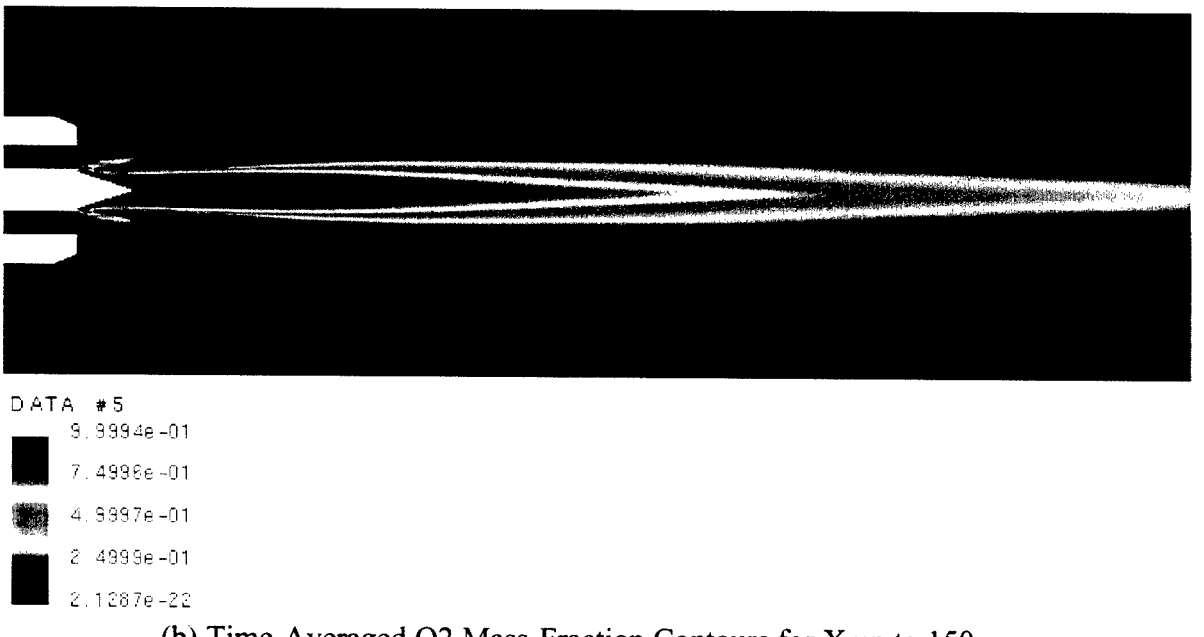

(b) Time-Averaged O2 Mass-Fraction Contours for X up to 150 mm

Figure 2. Time-Averaged OH and O_2 Mass Fractions of RCM-2.

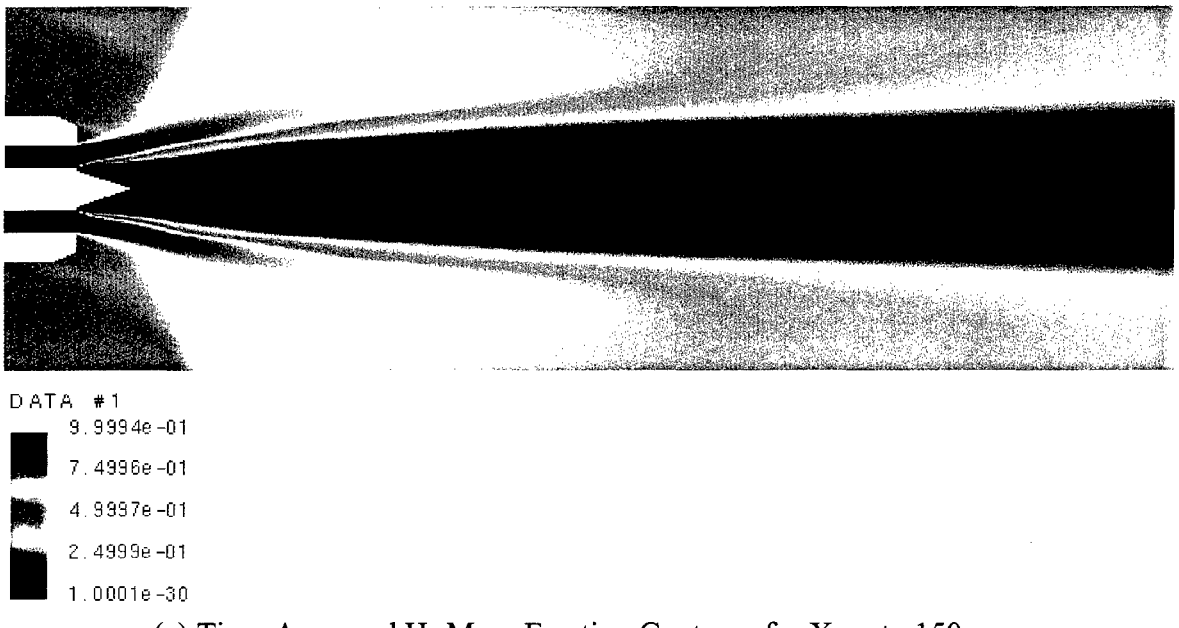

(a) Time-Averaged H_2 Mass-Fraction Contours for X up to 150 mm

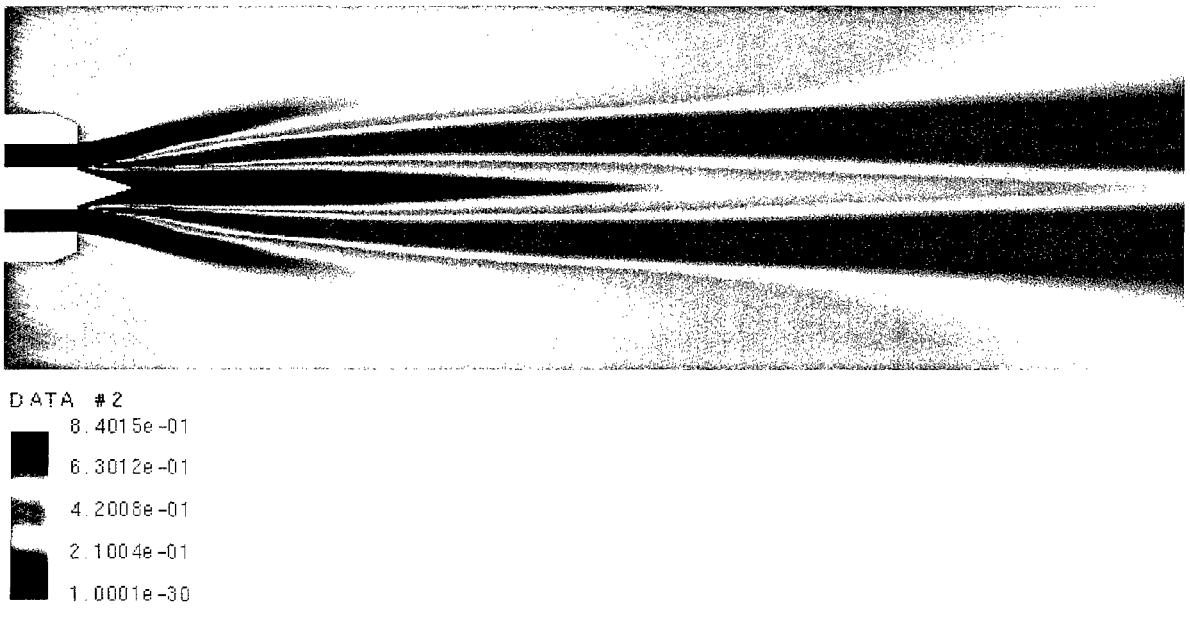

(b) Time-Averaged H_2O Mass-Fraction Contours for X up to 150 mm

Figure 3. Time-Averaged H_2 and H_2O Mass Fractions of RCM-2.

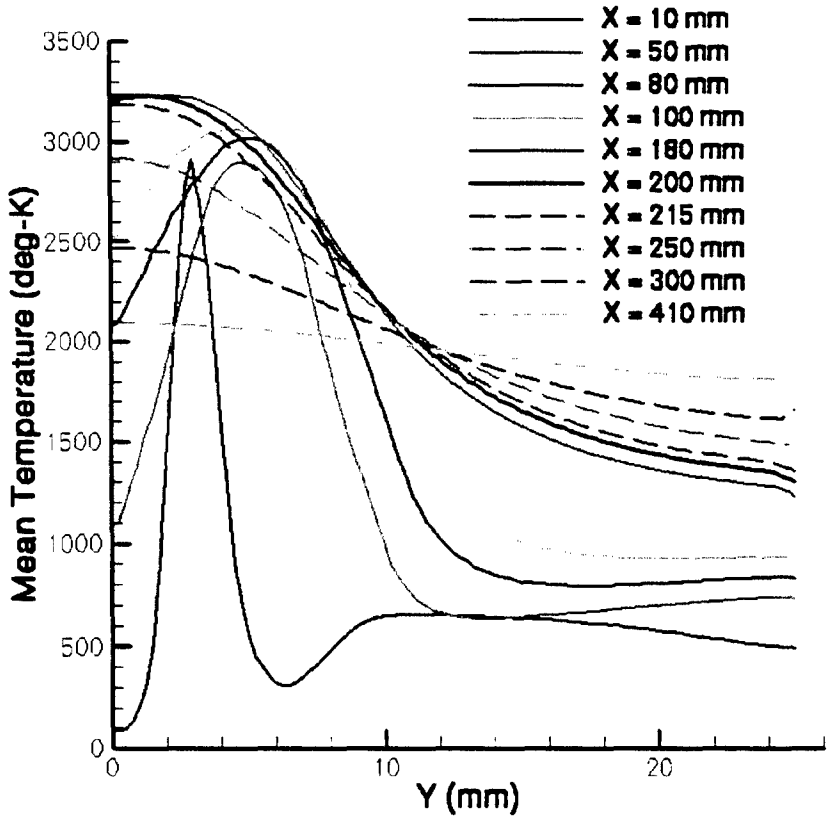

Figure 4. Predicted radial profiles of mean temperature of RCM-2.

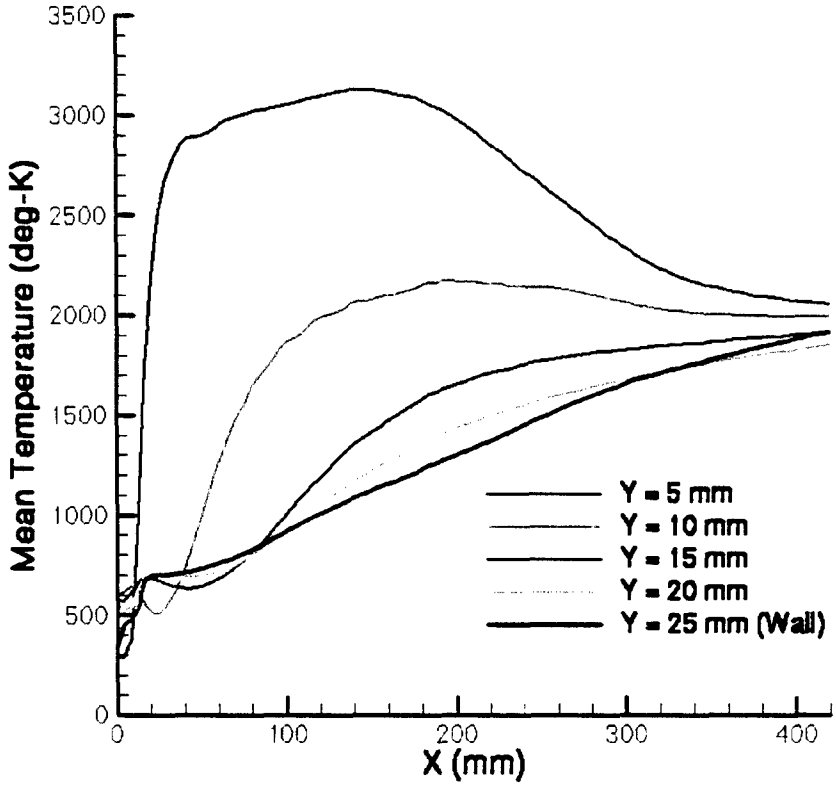

Figure 5. Predicted axial profiles of the mean temperature of RCM-2.

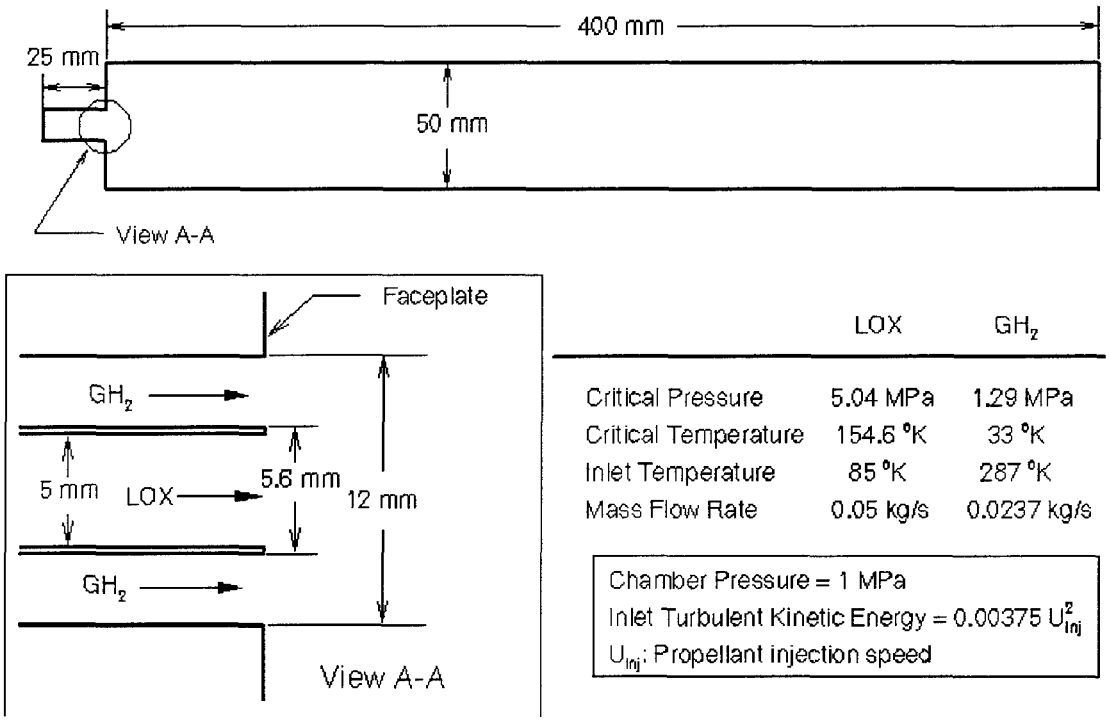

Figure 6. Configuration of the RCM-2 Case (Homogeneous Spray Model).

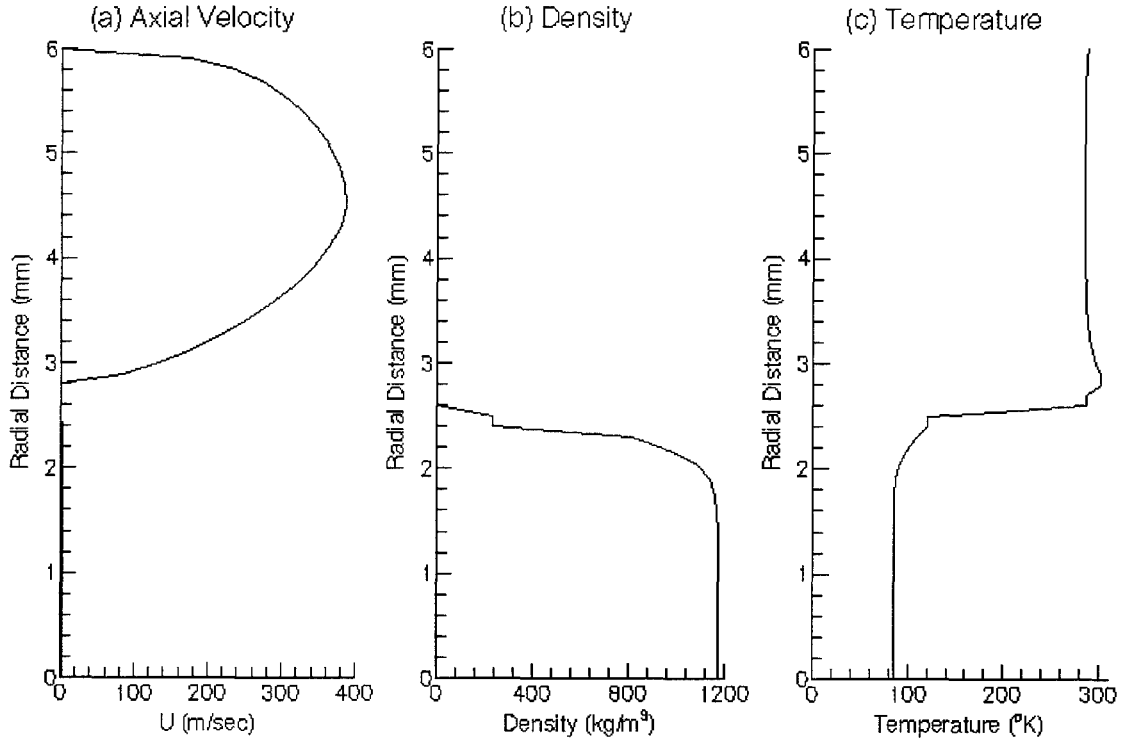

Figure 7. Flow Properties at the Injector Exit of RCM-2 (Homogeneous Spray Model)

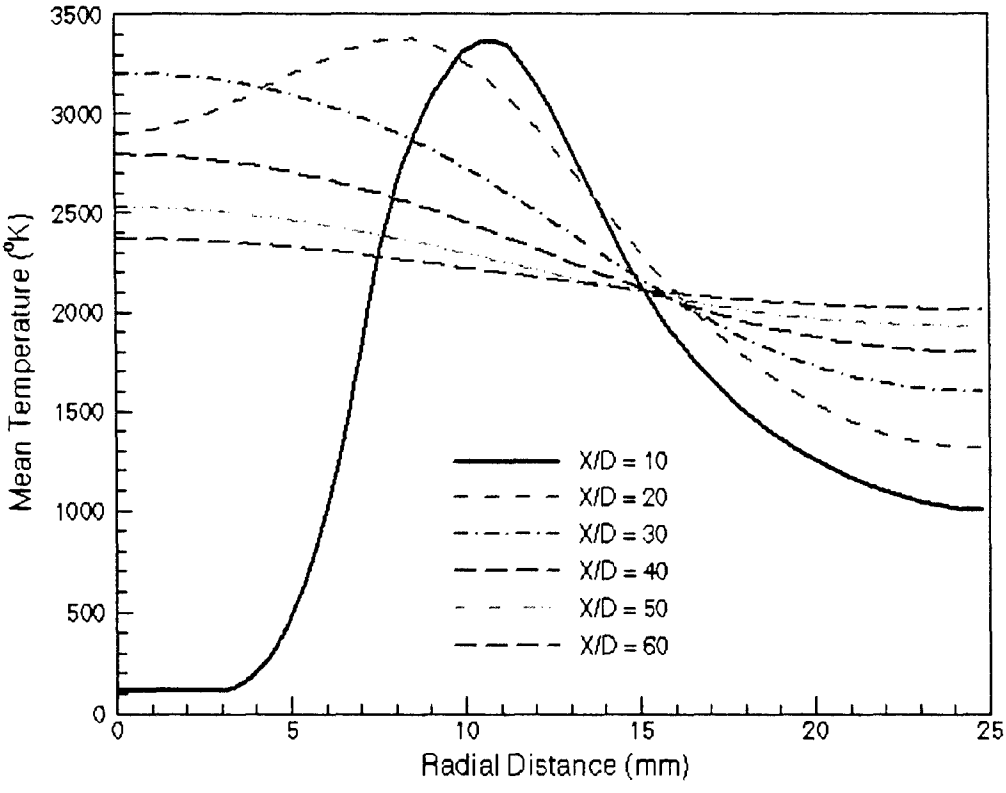

Figure 8. Radial Profiles of the Mean Temperature at Various Axial Locations of RCM-2.

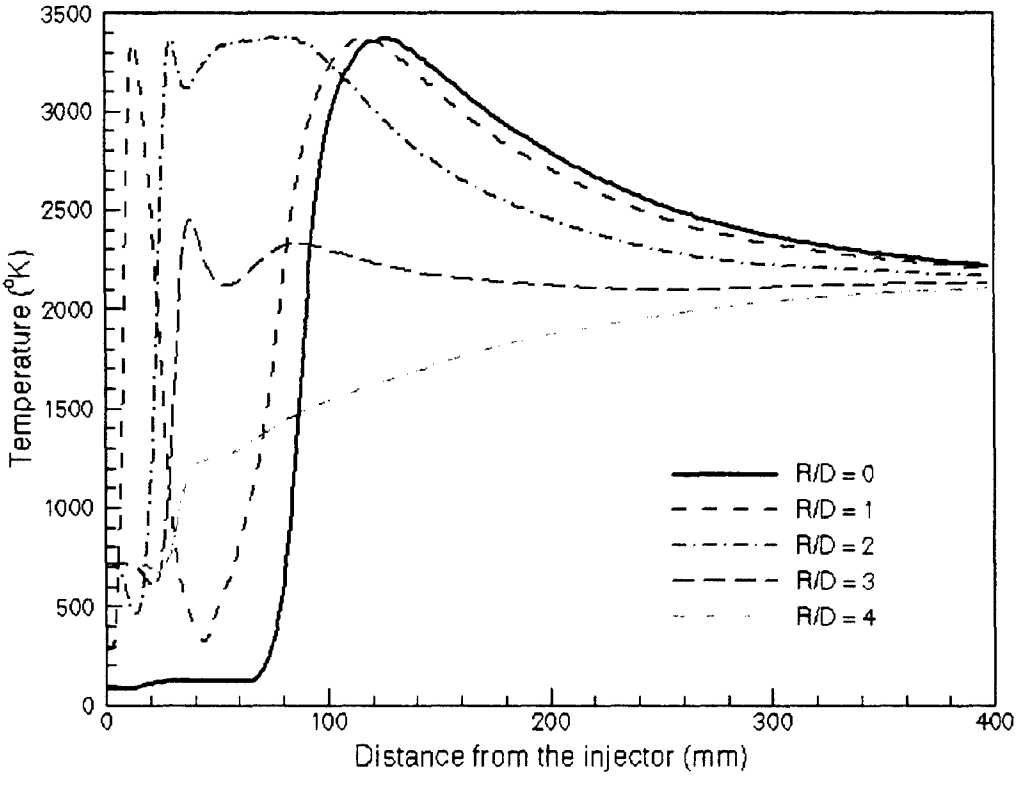

Figure 9. Axial Profiles of the Mean Temperature at Various Radial Locations of RCM-2.

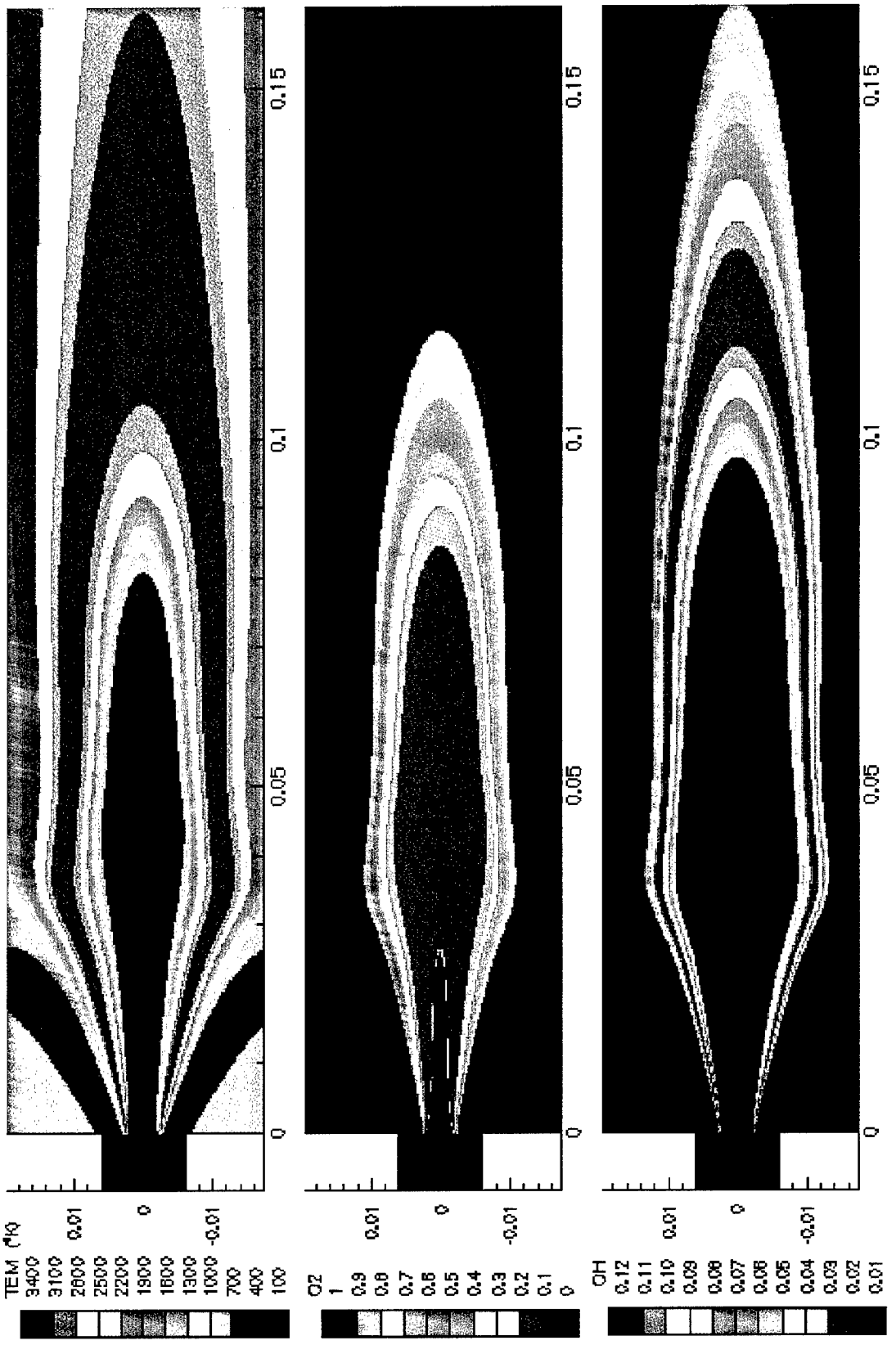

Figure 10. Temperature and Species Concentrations Near the Injector of RCM-2.

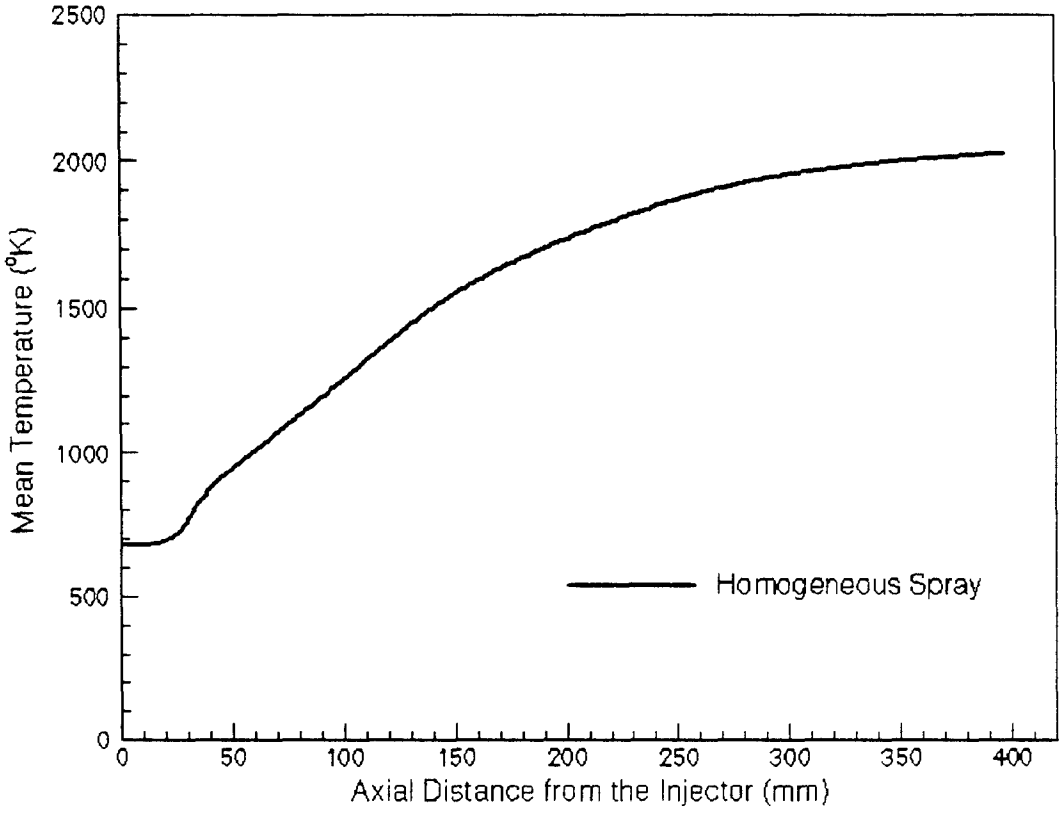

Figure 11. Near Wall Temperature Distributions for Various Chemistry Models of RCM-2.